Supplementary Material

for

A methylation-inspired mesoporous coordination polymer for identification and removal of organic pollutants in aqueous

Zhonghui Chen*[a,b] , Ziyu Lv [c], Zirong Lin [a], Jun Chen [a], Yifang Zhang [a], Cunli Wang [d], Guangyan Qing [d], Yifeng Sun *[a], Zhenguo Chi *[b]

a. Guangdong Provincial Public Laboratory of Analysis and Testing Technology, Guangdong Institute of Analysis (China National Analytical Center Guangzhou), Guangdong Academy of Sciences, Xianlie Road 100, Guangzhou 510070, China

b. Guangdong Engineering Technology Research Center for High-performance Organic and Polymer Photoelectric Functional Films, State Key Laboratory of OEMT, School of Chemistry, Sun Yat-sen University, Guangzhou 510275, China

c. Institute of Microscale Optoelectronics, Shenzhen University, Shenzhen 518060, China

d. Key Laboratory of Separation Science for Analytical Chemistry, Dalian Institute of Chemical Physics, Chinese Academy of Sciences, Dalian 116023, China

Correspondence to:

Chen_Zhonghui414@163.com; sunyifengly@163.com; chizhg@mail.sysu.edu.cn

Table of contents

1. Experimental details

1.1 Materials

All reagents and solvents used are commercially available grade and used without further purification. The amino acid Phe, dipeptides Phe-Phe, Asp-Phe are purchased from GL Biochem Ltd. (Shanghai, China), and Asp-Phe methyl ester was purchased from Macklin Biochemical Co., Ltd (Shanghai, China). Methanol, ethanol, copper (Ⅱ) acetate monohydrate and other chemicals were supplied from Guangzhou Chemical Reagent Factory (Guangzhou, China). Compared with previous methods[1-3], in order to create unsaturated sites and provide more binding sites for specific adsorption, four metal-bioligand complexes were prepared in a weak acidic mixture of methanol and water, with details as follows. Both commercial metal-organic frameworks UiO-66 and MIP-Zr(202) were purchased from Chemsoon cop. (Shanghai, China).

1.2 Synthetic procedures

1.2.1 Synthesis of CuF_2

L-Phenylalanine (0.148 g, 0.9 mmol) was dissolved in 12.6 mL water. After that, a copper acetate aqueous solution (0.3 M, 3 mL) was added to this clear colorless solution, the targeted light-blue powder was obtained immediately. Main FTIR features of L-phenylalanine are: 3352 cm^{-1} (s, νN-H of NH_2), 3105–2953 cm^{-1} (s, νC-H of the aromatic ring and aliphatic chain), 1732 cm^{-1} (m, νC=O of the carboxylic group), 1624 cm^{-1} (m, $\nu_{as}(-NH_3^+)$), 1547 cm^{-1} (s, $\nu_{as}(COO^-)$), 1495 cm^{-1} (s, $\nu_s(-NH_3^+)$), 1408 cm^{-1} (s, $\nu_s(COO^-)$) and 1306 cm^{-1} (s, νC-O of the carboxylic group). Main FTIR features of CuF_2 differ from those of the free L-phenylalanine with respect to the position and profile of some bands, indicating the participation of the corresponding groups in the coordination to the copper cation. The NH_2 stretching band decreases to 3331 and 3248 cm^{-1}, and asymmetrical vibration $-NH_3^+$ band decreases to 1614 cm^{-1}. The νC=O of carboxylic group in 1732 cm^{-1} is disappeared. Both the asymmetrical and symmetrical vibration COO^- bands of carboxylate group shift to 1573 and 1381 cm^{-1}, respectively; and νC-O of the carboxylic group shifts to 1321 cm^{-1}. Analysis. Calc. for CuF_2, $[CuC_{18}H_{20}N_2O_4]$ (Mw = 391.91): C, 55.11; N, 7.14; H, 5.10. Found: C, 54.87; N, 7.14; H, 5.21.

1.2.2 Synthesis of CuFF

L-Phenylalanyl-L-Phenylalanine (0.281 g, 0.9 mmol) was dispersed in 12.6 mL methanol by manual stir, then 3 mL copper acetate solution was added in. The white suspension was turned into a deep blue solution, and then left to stand in a temperature controlled chamber by slow evaporation at 85 °C for 48 h until the formation of blue fibrous crystals. Main FTIR features of L-phenylalanyl-L-phenylalanine are: 3252 cm^{-1} (s, νN-H of NH_2), 3061–2916 cm^{-1} (s, νC-H of the aromatic ring and aliphatic chain), 1688 cm^{-1} (s, νC=O of the amide group), 1612 cm^{-1} (s, νC=C of aromatic ring),

1551 cm^{-1} (s, δN-H, scissoring of NH_2), 1497 cm^{-1} (s, δC=C of the aromatic ring), 1431 cm^{-1} (m, δC-O-H of the carboxylic group), 1385 cm^{-1} (s, νC-O of the carboxylic group) and 1254 cm^{-1} (s, νC-N of the amide). Main FTIR features of CuFF differ from those of the free L-phenylalanyl-L-phenylalanine with respect to the position and profile of some bands, indicating the participation of the corresponding groups in the coordination to the copper cations. The NH_2 stretching band shifts to 3356 and 3281 cm^{-1}, and NH_2 scissoring band decreases to 1543 cm^{-1}. The C-O-H bending and C-O stretching bands (carboxylate group) change to 1437 and 1410 cm^{-1}, respectively. Asymmetric and symmetric stretching bands of the bridge bidentate carboxylate (M-O-C-O-M) at 1572 and 1410 cm^{-1}. Analysis. Calc. for Cu(FF), [$CuC_{18}H_{18}N_2O_3$] (Mw = 373.90): C, 57.77; N, 7.49; H, 4.81. Found: C, 57.41; N, 7.53; H, 4.84.

1.2.3 Synthesis of CuDF

L-Aspartyl-L-Phenylalanine (0.252 g, 0.9 mmol) and 3 mL copper acetate solution were mixed by sequential addition of 12.6 mL methanol and 2 mL water. The mixture was heated at 85 °C for 48 h, and then the blue powders were collected. Main FTIR features of L-Aspartyl-L-Phenylalanine are: 3549–3483 cm^{-1} (m, νO-H of carboxylic group), 3352 cm^{-1} (s, νN-H of NH_2), 3092–2891 cm^{-1} (m, νC-H of the aromatic ring and aliphatic chain), 1734 cm^{-1} (s, νC=O of the carboxylic group), 1672 cm^{-1} (s, νC=O of the amide group), 1543 cm^{-1} (s, δN-H, scissoring of NH_2), 1499 cm^{-1} (m, s, δC=C of the aromatic ring), 1423 cm^{-1} (m, δC-O-H of the carboxylic group), 1309 cm^{-1} (s, νC-O of the carboxylic group). Main FTIR features of CuDF differ from those of the free aspartame with respect to the position and profile of some bands, indicating the participation of the corresponding groups in the coordination to the copper cations. A strong band in 3549 cm^{-1} related to the O-H stretch and association of the carboxylic group is disappeared, both the NH_2 stretching and

scissoring band decreases to 3229 and 1537 cm^{-1}. The C-O-H bending and C-O stretching bands (carboxylate group) change to 1447 and 1394 cm^{-1}, respectively. Asymmetric and symmetric stretching bands of the bridge bidentate carboxylate (M-O-C-O-M) at 1601 and 1394 cm^{-1}. Analysis. Calc. for Cu(DF), [$CuC_{13}H_{14}N_2O_5$] (Mw = 341.81): C, 45.68; N, 8.20; H, 4.13. Found: C, 45.89; N, 8.01; H, 4.12.

1.2.4 Synthesis of Cu(mDF)

L-Asp-L-Phe methyl ester (0.265 g, 0.9 mmol) and 3 mL copper acetate solution were manually stirred by sequential addition of 12.6 mL methanol and 2 mL water for obtaining an ocean blue dispersion. After heating at 85 °C for 48 h, the blue powders was obtained. Main FTIR features of aspartame are: 3333 cm^{-1} (s, νN-H of NH_2), 3068–2856 cm^{-1} (s, νC-H of the aromatic ring and aliphatic chain), 1738 cm^{-1} (s, νC-H of the ester), 1666 cm^{-1} (s, νC=O of the amide group), 1585 cm^{-1} (s, νC=C of aromatic ring), 1547 cm^{-1} (s, δN-H, scissoring of NH_2), 1496 cm^{-1} (m, δC=C of the aromatic ring), 1446 cm^{-1} (m, δC-O-H of the carboxylic group), 1379 cm^{-1} (s, νC-O of the carboxylic group) and 1227 cm^{-1} (m, νC-O of the ester). Main FTIR features of CuFF differ from those of the free aspartame with respect to the position and profile of some bands, indicating the participation of the corresponding groups in the coordination to the copper cations. A strong band in 3356 cm^{-1} is related to the O-H stretch of the coordinated water molecule, and both NH_2 stretching and scissoring band decreases to 3230 and 1539 cm^{-1}. The C-O-H bending and C-O stretching bands (carboxylate group) change to 1448 and 1398 cm^{-1}, respectively. Asymmetric and symmetric stretching bands of the bridge bidentate carboxylate (M-O-C-O-M) at 1614 and 1398 cm^{-1}. Analysis. Calc. for Cu(mDF), [$CuC_{14}H_{16}N_2O_5$] (Mw = 355.84): C, 47.26; N, 7.87; H, 4.53. Found: C, 44.89; N, 7.95; H, 4.21.

All the products were centrifuged, and washed with water and absolute methanol three times respectively, then dried at 85 °C for removing the solvent and stored in glass vials at 4 °C.

2. Methods

2.1 Characterization

Scanning electron microscopy (SEM, Hitachi S-3700N) was used to observe the morphology of products. Surface and pore size analyzer (Micromeritics® ASAP2460) was used to record the N_2 adsorption-desorption curves of solids. PXRD patterns of products were collected in Rigaku Ultima Ⅳ diffractometer using copper radiation (Cu Kα = 1.5418 Å), operating at 40 mA and 45kV. Profiles were collected in the $3° < 2\theta < 60°$ range with a step size of 0.02°. Variable temperature trials were performed in a SmartLab X-Ray diffractometer (Rigaku, Japan) using a Pt heater in N_2 atmosphere. Data were collected between 3 and 60° 2θ, and then every 30 °C between 30 and 180 °C. The temperature was changed with a heating rate of 10 °C·min^{-1} and allowed to equilibrate for 2 min prior to data collection. After being treated under vacuum for 24 h, the samples were analyzed by X-ray photoelectron spectroscopy (XPS, ESCALAB 250Xi). Fourier transform infrared spectra (FTIR) measurements were accomplished by a Bruker Vertex 80v infrared spectrophotometer in the frequency range 400 – 4000 cm^{-1}. Thermalgravimetric measurements were performed in a N_2 atmosphere using a simultaneous TG-DSC (Netzsch STA499) thermal analyzer in the temperature range of 25 – 800 °C. The heating rate was 10 K·min^{-1}. The elemental analysis was performed using Thermo Flash EA 1112 apparatus. Zeta potential results were carried on a Malvern Zetasizer Nano ZS90; 5 mg of particles were dosed in 10 mL of aqueous solution with various pH values from 2 to 11. All the samples were put in the ultrasonic bath for 30 min before testing, and solution pHs were adjusted by 0.1 M HCl or NaOH diluted solution.

2.2 Stability of Cu-based coordination polymers

Inductively coupled plasma mass spectrometry (ICP-MS, Agilent 7700) was employed to monitor the Cu^{2+} released from four samples.[4] 5 mg·mL^{-1} samples were suspended in sodium chloride solution (0.9% wt.), and the mixture was stirred at room temperature. The concentrations of leaking Cu^{2+} in the mixture solution were recorded after time intervals of 6 h, 12 h, 24 h and 48 h.

2.3 Static adsorption efficiency studies**.**

Adsorption kinetic study[5] was performed in 3.5 mL quartz colorimetric dish by UV-vis spectroscopy (Hitachi U-4100) at room temperature. 3 mg sample was initially soaked with H_2O and then transferred to the dish. Then a 3 mL pollutant stock solution was added. The concentrations of pollutants in stock solutions were characterized by UV-vis spectroscopy, which were determined for methyl red (MR, 50 μM, at λmax = 514 nm, aqueous solution), bromophenol blue (BPB, 10 μM, at λmax = 590 nm, aqueous solution), bisphenol A (BPA, 200 μM, at λmax = 280 nm, aqueous solution), methylene blue (MB, 10 μM, at λmax = 664 nm, aqueous solution), 4, 4'-sulfonyldiphenol (SDP, 50 μM, at λmax = 260 nm, ethanol solution), and 4, 4'-sulphonybis (2, 6-dibromophenol) (TBS, 67.2 μM, at λmax = 268 nm, ethanol solution). Identical concentrations (1 mg·mL^{-1}) of Cu(mDF) powders were soaked in the water/ethanol mixtures or ethanol containing different dyes. And corresponding UV/Vis absorbance changes of supernatants were monitored after 0, 3, 7, 10, 15, 20, 30, 60 min.

The efficiency of organic pollutant removal by the sorbent was determined by the following equation[6]:

$$Pollutant\ removal\ efficiency = \frac{C_0 - C_t}{C_0} \times 100\%$$

where C_0 and C_t are the initial and residual concentration of pollutant in the solution before and after adsorption for t min.

The amount of organic pollutant adsorbed by the sorbent was determined by the following equation:

$$q_t = \frac{(C_0 - C_t)M_W}{m}$$

where qt (μg·mg^{-1}) is the amount of pollutant adsorbed per mg of sorbent at time t (min), m (mg) is the mass of sorbent used in the study. Mw is the molar mass of the organic pollutant.

2.4 Quick adsorption efficiency studies

The λmax of organic dyes in stock solutions were characterized by 722N visible spectrophotometer, which were determined for erythrosine B (AR51, 20 μM, at λmax = 526 nm), ponceau 4R (P4R, 20 μM, at λmax = 524 nm), methyl red (MR, 50 μM, at λmax = 514 nm), amaranth (AR, 20 μM, at λmax = 520 nm), sunset yellow (SY, 30 μM, at λmax = 482 nm), lemon yellow (LY, 20 μM, at λmax = 436 nm), brilliant blue (BB, 10 μM, at λmax = 628 nm), indigo blue (IB, 500 μM, at λmax = 582 nm), bromophenol blue (BPB, 40 μM, at λmax = 590 nm), methylene blue (MB, 20 μM, at λmax = 664 nm). Aqueous solutions of dyes mixing with each adsorbents (1 mg·mL^{-1}) were sufficiently blended by vortex for 1 min, then suspensions were centrifuged at 4000 rpm for 5 min and supernatants were removed for spectrum detection. Dyes were dissolved in a mixture of water/ethanol (*v* : *v* = 99 : 1). A small amount of ethanol was added to improve the dispersion of the hydrophobic powders in water.

2.5 Antimicrobial property studies

Four types of bacteria including Candida albicans, Escherichia coli, Staphylococcus aureus, and Salmonella enterica serovar typhimurium, were used to evaluate the antimicrobial activity of Cu(mDF) discs and cultured in the Sabouraud's dextrose agar (SDA, for the fungus, Candida albicans) or nutrient agar (NA, for the bacteria, including E. coli, S. aureus and S. typhimurium) culture medium, respectively. The experiments were conducted by the standard of GB

21551.2–2010 “antibacterial and cleaning function for household and similar electrical appliances–particular requirements of material”. The technical criteria accorded with requirement except for our test samples with smaller sizes. All the specimens used for antimicrobial tests were sterilized under ultraviolet light for 8 h. In experiment group, 0.1 g of Cu(mDF) powder was pressed into a disc with a diameter of 18 mm and a thickness of 0.45 ± 0.5 mm. Similar-sized healthy-grade high-density polyethylene (HDPE) discs were used in controlled trials. The concentration of the initial inoculum was 10^5 of the number of colony forming units (CFU) mL^{-1}. 200 μL of initial bacterial suspension was incubated on HDPE discs (control) and Cu(mDF) discs, respectively. The samples were covered by sterilized film to uniformly contact with bacteria, and then incubated at 37 °C in a relative humidity above 90%. After incubation for 24 h, the diluted bacterial solutions were obtained by drip washing the samples with 20 mL eluent, and then seeded in culture medium for another 24 h. The numbers of bacterial viable colonies were counted for determination of CFUs presented in each samples.

The antimicrobial ratio of the Cu(mDF) was determined by the following equation:

$$R = \frac{B - A}{B} \times 100\%$$

where R is antimicrobial ratio of Cu(mDF), B and A are the mean average of bacteria count for HDPE samples (control group) and Cu(mDF) samples (experiment group), respectively.

2.6 *In-vitro* cytotoxicity studies

The cytotoxicity of Cu(mDF) powders to mouse neuroblastoma N2a cells (a common cell model for *in-vitro* pathological study) was evaluated using CCK-8 assay by the extraction dilution method. Firstly, 0.1 $mg \cdot mL^{-1}$ of sterilized Cu(mDF) powders was soaked in high glucose DMEM culture solution (GIBCO BRL, NY, USA) supplemented with 10% fetal bovine serum (FBS, GIBCO BRL),

0.9% saline solution at 37 °C for 24 h. After filtration with a 0.22 μm pore size hydrophilic PES membrane (JET BIOFIL, Guangzhou, China), the extraction was diluted with culture medium in 1:2, 1:5, 1:20, 1:50 volume ratios for cytotoxicity assessment. N2a cells were cultured in high glucose DMEM medium supplemented with 10% FBS and 1% penicillin-streptomycin (GIBCO BRL) at 37 °C and 5% CO_2 in a humid environment. Once the cells reached 95% confluence and digested by 0.25% trypsin-EDTA, the cells were collected and seeded in 96-well microculture plates at a density of 5×10^3 cells/well in 100 μL complete culture medium. After 48 h, the medium was replaced with the diluted extracts and then the cells were incubated for another 24 h. After incubation, each well was washed with PBS twice and the CCK-8 reagent was added to each well according to the operation guidance. The absorbance of each well was measured at 450 nm using an automatic microplate reader (Spectra Max 340, Molecular Device Inc., USA). Relative cell viability was defined as the percentage of the optical density of a diluted extract containing medium to the optical density of the corresponding non-treated control. Each experiment had been repeated three times. For solution based assays, the error bars represent standard deviations of the average of three independent experiments.

3. Characterization data

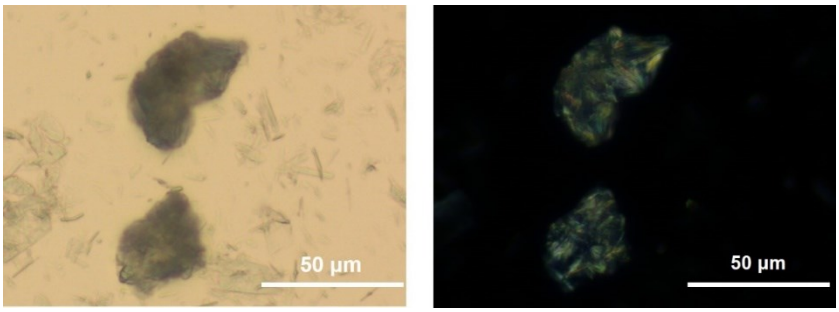

Figure S1. Optical images of as-prepared CuF_2 studied by polarizing microscope (PLM) with polarized light (left) and perpendicular polarized light (right).

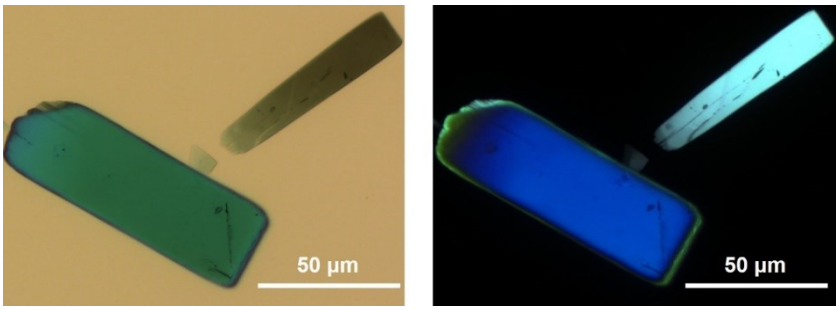

Figure S2. Optical images of as-prepared CuFF studied by PLM with polarized light (left) and perpendicular polarized light (right).

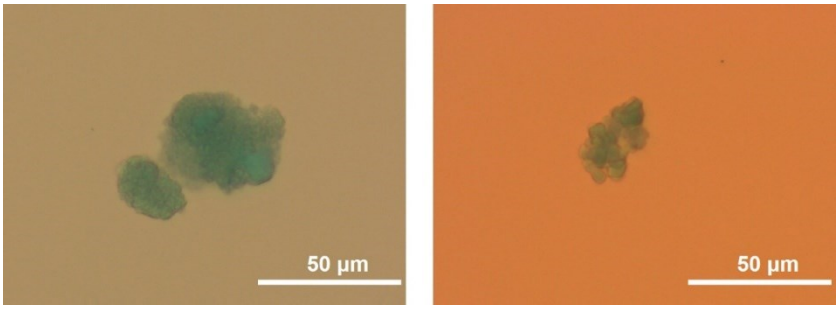

Figure S3. Optical images of as prepared CuDF (left) and Cu(mDF) (right) by PLM with polarized light.

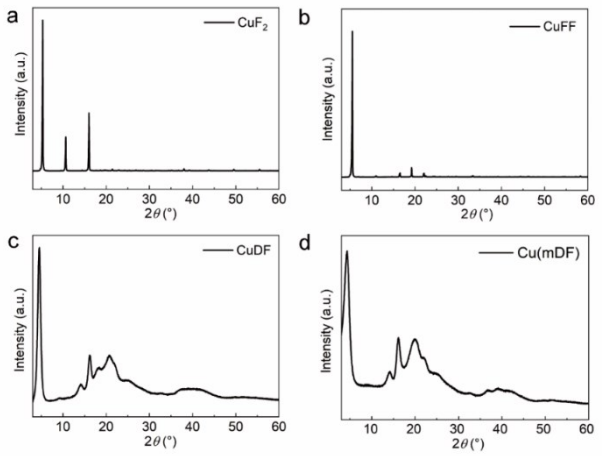

Figure S4. Powder X-ray diffraction patterns (PXRD) of four samples, (a) CuF_2, (b) CuFF, (c) CuDF, (d) Cu(mDF).

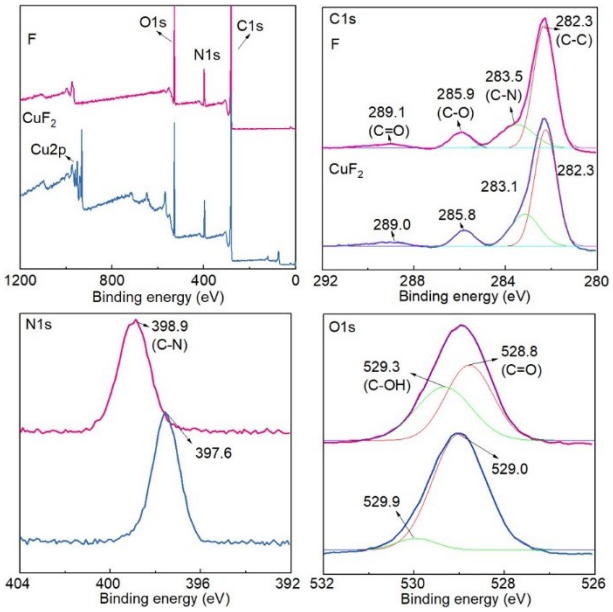

Figure S5. X-ray photoelectron spectra (XPS) of F and CuF_2, and their corresponding C1s, N1s, and O1s spectra. The existence of Cu2p peaks, the C1s spectra (C=O, 289.1 eV; C-O, 285.9 eV; C-N, 283.5 eV) shifting to the lower values (C=O, 289.0 eV; C-O, 285.8 eV; C-N, 283.1 eV), along with N1s (amino, 398.9 to 397.6 eV); and up-shifting of the O1s binding energy (C=O, 528.8 to 529.0; C-OH, 529.3 to 529.9 eV) can be attributed to the formation of Cu-F complex.

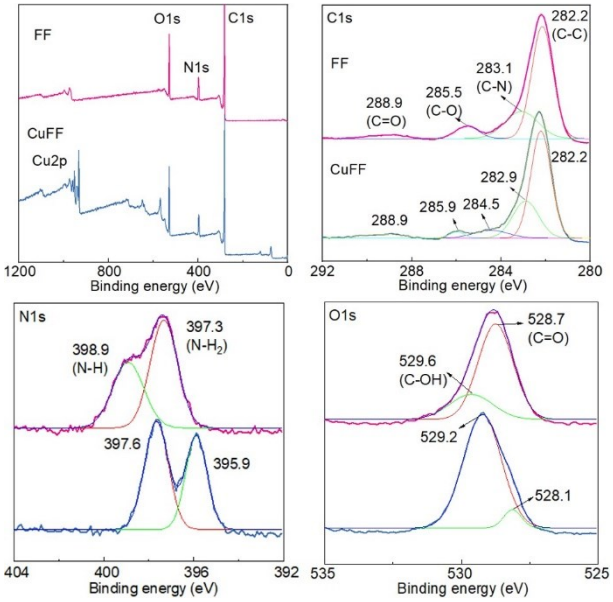

Figure S6. X-ray photoelectron spectra (XPS) of FF and CuFF, and their corresponding C1s, N1s, and O1s spectra. The existence of Cu2p peaks, the C1s spectra (C-O, 285.5 eV; C-N, 283.1 eV) shifting to the values (carboxyl C-O, 284.5 eV; C-N, 282.9 eV), along with the N1s spectra (amide, 398.9 to 397.6 eV; amino, 397.3 to 395.9 eV); the up-shifting of the broad O1s peaks (carboxyl C-OH and amide C=O) can be attributed to the formation of Cu-F complex.

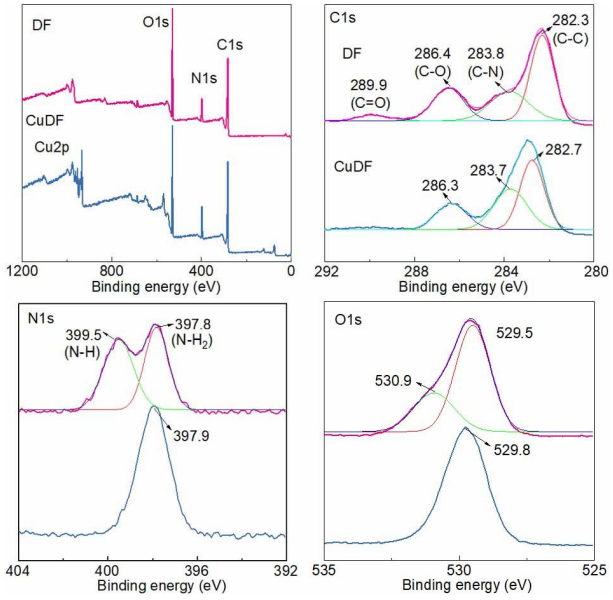

Figure S7. X-ray photoelectron spectra (XPS) of DF and CuDF, and their corresponding C1s, N1s, and O1s spectra. The existence of Cu2p peaks, the C1s spectra (C-O, 286.4 eV; C-N, 283.8 eV; C-C, 282.3 eV) shifting to the values (carboxyl C-O, 286.3 eV; C-N, 283.7 eV; C-C, 282.7 eV), along with the N1s peaks (amide, 399.5; amino, 397.8 eV) merging into a broad peak (397.9 eV), as well as two O1s peaks (carboxyl C-OH, 530.9 eV; amide C=O, 529.5 eV) merging into a broad peak (529.8 eV) can be attributed to the formation of Cu-DF complex.

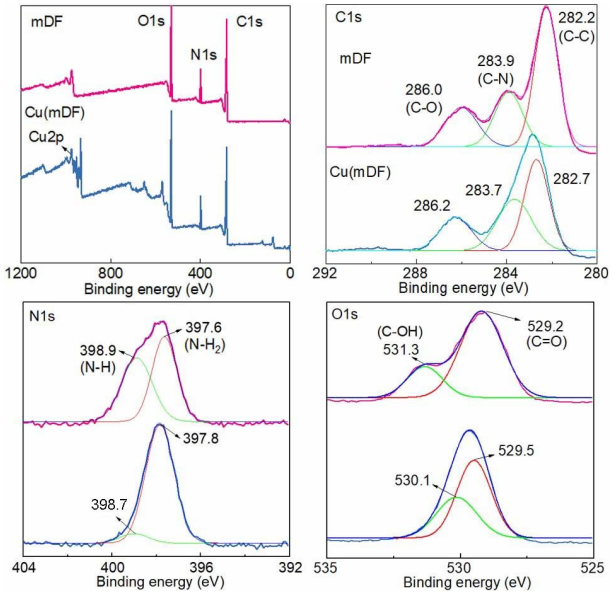

Figure S8. X-ray photoelectron spectra (XPS) of mDF and Cu(mDF), and their corresponding C1s, N1s, and O1s spectra. The existence of Cu2p peaks, the C1s spectra (C-O, 286.0 eV; C-N, 283.9 eV; C-C, 282.2 eV) shifting to the values (carboxyl C-O, 286.2 eV; C-N, 283.7 eV; C-C, 282.7 eV), along with the N1s peaks (amide, 398.9; amino, 397.6 eV) merging into a broad peak (397.8 eV), as well as two O1s peaks (carboxyl C-OH, 531.3 eV; amide C=O, 529.2 eV) merging into a broad peak (C-OH, 530.1 eV; C=O, 529.5 eV) can be attributed to the formation of Cu-mDF complex.

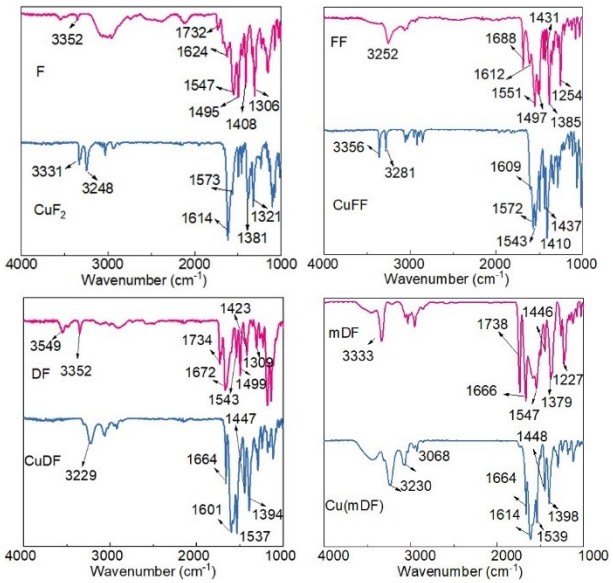

Figure S9. FT-IR spectra of four samples in the 4000–1000 cm^{-1} range from as-prepared powders diluted in KBr pellets, (a) CuF_2, (b) CuFF, (c) CuDF, (d) Cu(mDF).

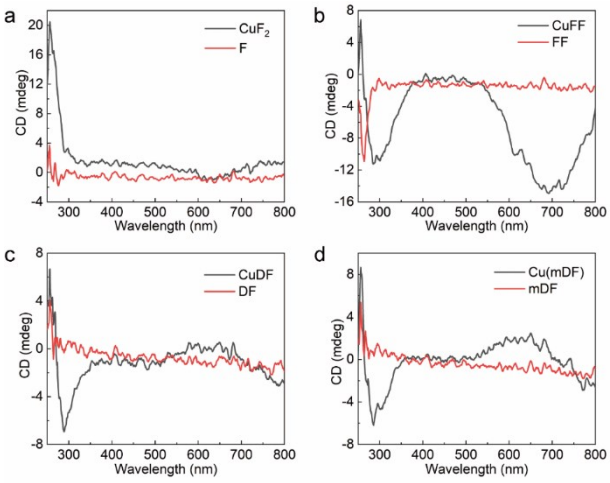

Figure S10. Solid-state chiral dichroism (CD) UV-Vis spectra of four bioligands (black) and corresponding coordination polymers (red). Spectra was collected with a spectropolarimeter Jasco J-810 and recorded at a temperature of 25 °C. Ellipticity values were recorded every 1 nm at a wavelength scanning speed of 20 nm/min. The response time was set to 1 s and the bandwidth was set to 1 nm. The final spectrum represented the accumulate average of three consecutive scans.

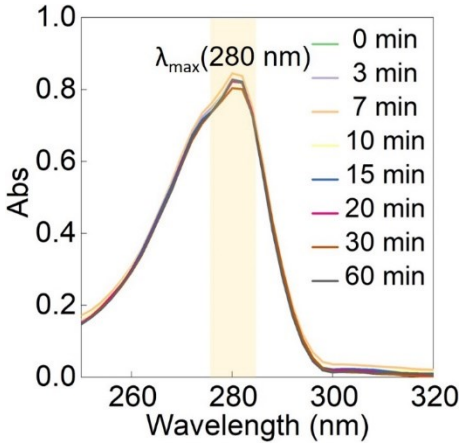

Figure S11. Time-dependent adsorption of bisphenol A in ethanol solution by Cu(mDF) characterized by UV-vis spectra.

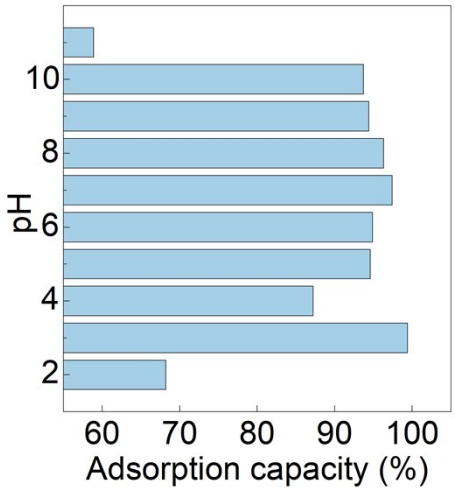

Figure S12. Adsorption capacity of bromophenol blue in the pH ranges of 2 to 11. As BPB is a pH indicator, pH value influences the color of BPB. The maximum UV adsorption wavelength of BPB is determined at 438 nm below the pH 4, and at 590 nm above the pH 4, respectively.

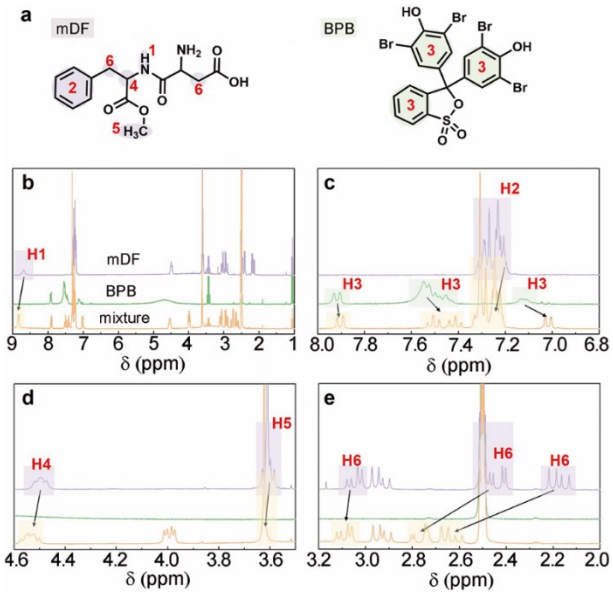

Figure S13. (a) Structure of mDF and BPB marked with the protons participating in binding affinities. (b-e) Partial ^{1}H NMR spectra (DMSO-d6, 400MHz, rt) of the mDF, BPB and their mixture in ratio of 1 : 1.

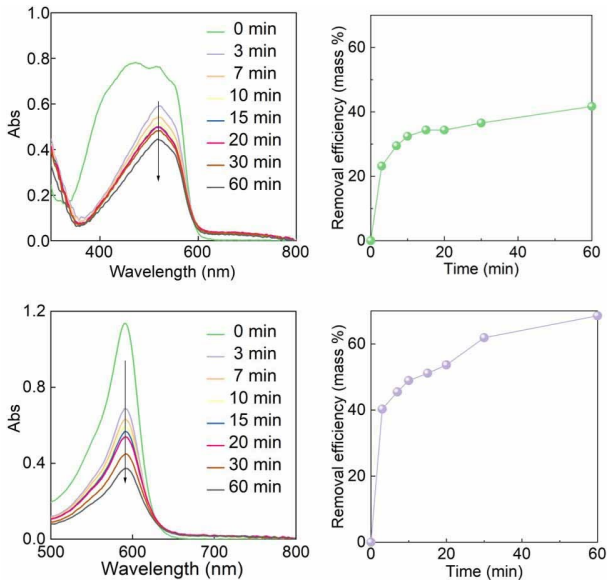

Figure S14. Characterization of MR (up) and BPB (down) uptake by CuDF adsorbent. UV-vis spectra recorded as a function of immersion time with CuDF (1 mg mL^{-1}), and their corresponding time-dependent removal efficiency by CuDF.

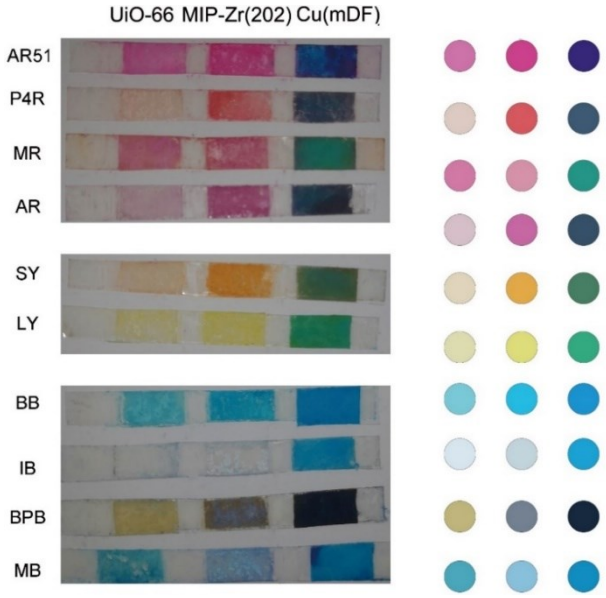

Figure S15. Hand-made test strip composed of three adsorbents, including UiO-66, MIP-Zr(202) and Cu(mDF), fixed at intervals. Photographs of the test strips after insertion into different dye solutions (left), and corresponding color circles after sample dry. For images, the color was determined by the color sampler tool (right) in Photoshop software, and the sample area size was set to 31 × 31 pixels (average).

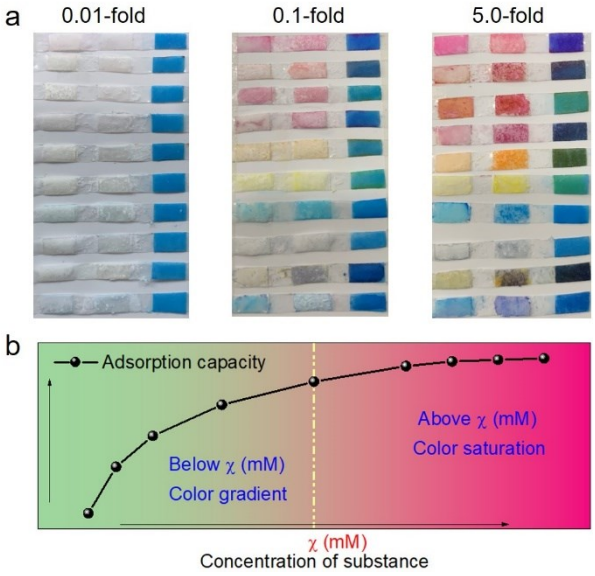

Figure S16. (a) Hand-made strips testing results in 0.01-fold, 0.1-fold and 5.0-fold of different dye solutions. (b) The relationship model between the adsorption capacity of adsorbents and initial testing concentration of adsorbate.

4. References

1. Lively, R. P.; Sholl, D. S. From water to organics in membrane separations. Nat. Mater. 2017, 16, 276-279.

2. Lu, J.; Zhang, H.; Hou, J.; Li, X.; Hu, X.; Hu, Y.; Easton, C. D.; Li, Q.; Sun, C.; Thornton, A. W.; Hill, M. R.; Zhang, X.; Jiang, G.; Liu, J. Z.; Hill, A. J.; Freeman, B. D.; Jiang, L.; Wang, H. Efficient metal ion sieving in rectifying subnanochannels enabled by metal-organic frameworks. Nat. Mater. 2020, 19, 767-774.

3. Peng, J.; Wu, R. Metal-organic frameworks in proteomics/peptidomics - a review. Anal. Chim. Acta 2018, 1027, 9-21.

4. Cavicchioli, M.; Massabni, A. C.; da Costa Ferreira, A. M.; Castellano, E. E.; Crespi, M. S. Synthesis, structure and redox properties of an unexpected trinuclear copper(II) complex with aspartame: $[Cu(apm)_2Cu(\mu\text{-}N,O:O'\text{-}apm)_2(H_2O)Cu(apm)_2(H_2O)] \cdot 5H_2O$. Inorg. Chim. Acta 2005, 358, 4431-4436.

5. Facchin, G.; Kremer, E.; Baran, E. J.; Castellano, E. E.; Piro, O. E.; Ellena, J.; Costa-Filho, A. J.; Torre, M. H. Structural characterization of a series of new Cu-dipeptide complexes in solid state and in solution. Polyhedron 2006, 25, 2597-2604.

6. Stanila, A.; Marcu, A.; Rusu, D.; Rusu, M.; David, L. Spectroscopic studies of some copper(II) complexes with amino acids. J. Mol. Struct. 2007, 834, 364-368.